J|A|C|S COMMUNICATIONS

Published on Web 08/31/2010

Comprehensive Solid-State NMR Characterization of Electronic Structure in Ditechnetium Heptoxide

Herman Cho,*,† Wibe A. de Jong,‡ Alfred P. Sattelberger,§,|| Frédéric Poineau,|| and Kenneth R. Czerwinski||

Fundamental and Computational Sciences Directorate and Environmental Molecular Sciences Laboratory, Pacific Northwest National Laboratory, P.O. Box 999, Richland, Washington 99352, Energy Engineering and Systems Analysis Directorate, Argonne National Laboratory, Argonne, Illinois 60439, and Department of Chemistry and Harry Reid Center for Environmental Studies, University of Nevada Las Vegas, 4505 Maryland Parkway, Las Vegas, Nevada 89154

Received June 28, 2010; E-mail: hm.cho@pnl.gov

Abstract: A relativistic density functional theory description of the electronic structure of Tc_2O_7 has been evaluated by comparison with solid-state ^{99}Tc and ^{17}O NMR spectroscopic data (the former isotope is a weak β emitter). Every site in the molecule can be populated by a nucleus with favorable NMR characteristics, providing the rare opportunity to obtain a comprehensive set of chemical shift and electric field gradient tensors for a small molecular transition-metal oxide. NMR parameters were computed for the central molecule of a $(Tc_2O_7)_{17}$ cluster using standard ZORA-optimized all-electron QZ4P basis sets for the central molecule and DZ basis sets for the surrounding atoms. The magnitudes of the predicted tensor principal values appear to be uniformly larger than those observed experimentally, but the discrepancies were within the accuracy of the approximation methods used. The convergence of the calculated and measured NMR data suggests that the theoretical analysis has validity for the quantitative understanding of structural, magnetic, and chemical properties of Tc(VII) oxides in condensed phases.

The solid-state structures of Tc_2O_7 and Re_2O_7 feature a distinctive linear oxo bridge and pyramidal $-MO_3$ end groups.[1−3] These heptavalent oxides are also notable for displaying weak temperature-independent paramagnetism (TIP) despite having d^0 electronic configurations.[4] In the case of Tc_2O_7, the favorable properties of the 100%-abundant ^{99}Tc isotope ($I = {}^9/_2$; $\gamma = 9.583 \times 2\pi \times 10^6$ rad s^{-1} T^{-1}) and the ability to synthesize samples with ^{17}O enrichment make it possible to measure the electric field gradient (EFG) and chemical shift tensors of every atom in the molecule by solid-state NMR spectroscopy. Such data provide an excellent basis for determining the electron distributions and states of this molecular transition-metal oxide in its entirety.

Room-temperature spectra of polycrystalline Tc_2O_7 with and without ^{17}O enrichment were recorded in a magnetic field of 7.04 T [$\nu_L(^{99}Tc) = 67.565$ MHz; $\nu_L(^{17}O) = 40.722$ MHz], and the results were compared to theoretical predictions (Figures 1 and 2). The dominant feature in both sets of spectra is the ${}^1/_2 \leftrightarrow -{}^1/_2$ powder line shape. The simulated line shapes are functions of the nuclide's EFG and chemical shift tensors (Table 1) and the three Euler angles relating the principal axes of the two tensors. Methods for computing spectra given these inputs have been described previously.[7]

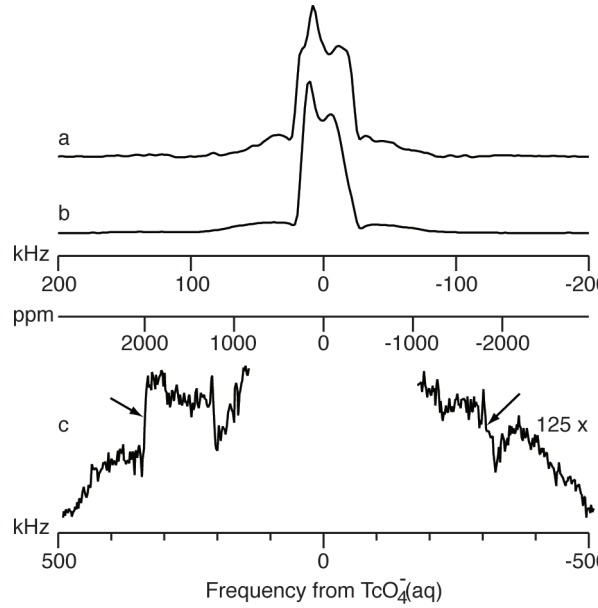

Figure 1. (a) Predicted and (b, c) experimental ^{99}Tc powder spectra of Tc_2O_7 with natural oxygen isotope levels. Spectrum (a) was computed with nonideal pulse parameters matching those used in the experiment. The arrows in (c) point to features assigned to the extreme shoulders of the ${}^3/_2 \leftrightarrow {}^1/_2$ powder line shapes.

Shielding and EFG tensors and scalar coupling constants were computed with the Amsterdam Density Functional (ADF version 2008.01) software[8] using the spin−orbit zeroth-order relativistic approximation (ZORA)[9] and the Perdew91 generalized gradient approximation density functional.[10] Calculations with a simple local density functional yielded results similar to Perdew91. The modeled system was a cluster of 17 molecules (153 atoms) based on the structure data of Krebs.[3] NMR properties were calculated for the central molecule of the cluster (Figure S2 in the Supporting Information) using standard ZORA-optimized all-electron QZ4P basis sets, while the surrounding atoms were described by DZ basis sets with a frozen core up to 1s and 3d for O and Tc, respectively. The numerical integration accuracy parameter was set to 6.0 throughout. Shielding values for nuclei in the reference compounds were obtained with the same Perdew91 and QZ4P basis sets, and the aqueous solution environment was approximated using the COSMO model[11] with a dielectric constant of 78.8 and radii

† Fundamental and Computational Sciences Directorate, Pacific Northwest National Laboratory.
‡ Environmental Molecular Sciences Laboratory, Pacific Northwest National Laboratory.
§ Argonne National Laboratory.
|| University of Nevada Las Vegas.

10.1021/ja105687j

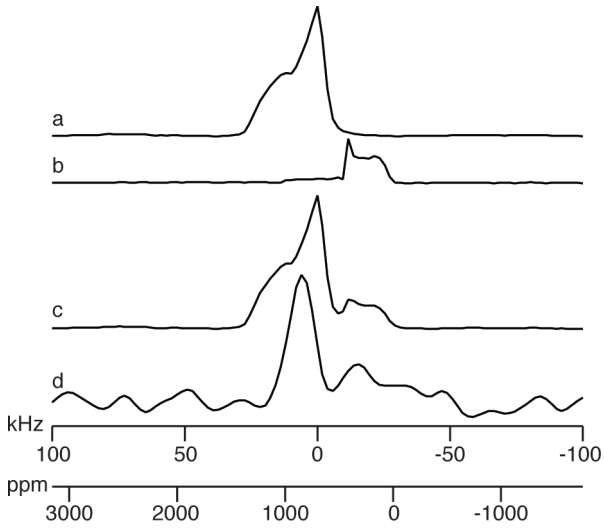

Figure 2. (a−c) Predicted and (d) experimental ^{17}O powder spectra of ^{17}O-enriched Tc_2O_7. The predicted spectra correspond to (a) the six terminal oxygens, (b) the single bridging oxygen, and (c) the superposition of all seven oxygens. Simulations were computed with parameters identical to those in the experiments, including finite pulse widths. The ppm scale is referenced to H_2O, and the kHz scale is centered on the spectrometer carrier frequency at 700 ppm.

Table 1. Computed NMR Tensor Parameters for the Centrosymmetric Central Molecule of a $(Tc_2O_7)_{17}$ Cluster

	EFG tensor data[a]		chemical shift tensor data (ppm)[b]		
atom	V_{zz} (10^{21} V/m^2)	η_Q	δ_{xx}	δ_{yy}	δ_{zz}
Tc	2.737	0.92	327	172	−282
O (bridge)	10.302	0.03	167	210	337
O (1.649)[c]	−4.609	0.83	681	799	1285
O (1.673)[c]	−5.269	0.73	712	849	1365
O (1.695)[c]	−5.555	0.66	633	843	1339

[a] V_{zz} and η_Q are defined according to Cohen and Reif.[5] [b] Referenced to solvated TcO_4^- [$\sigma_{iso}(^{99}Tc) = -1288$ ppm] or H_2O [$\sigma_{iso}(^{17}O) = 243$ ppm]. The ordering of the shift tensor principal values δ_{jj} follows Haeberlen.[6] [c] Distance of terminal oxygen to Tc (Å).[3]

defining the cavity surface equal to 1.85 for Tc, 1.55 for O, 1.20 for H, and 1.40 for the spherical solvent radius.

The experimental and simulated ^{99}Tc spectra are in good agreement with respect to the shape and position of the ^{99}Tc central transition powder resonance. The broader width of (a) relative to (b) indicates that the calculated chemical shift anisotropy and asymmetry parameter are slightly too large. Magnification of the experimental spectrum reveals symmetrically placed steplike features that appear to be the extrema of the $\pm^3/_2 \leftrightarrow \pm^1/_2$ powder line shapes. Although these steps are far removed from the spectrometer frequency, observable coherences of the ($\pm^3/_2$, $\pm^1/_2$) pairs of states can be indirectly excited through on-resonance irradiation of the $+^1/_2 \leftrightarrow -^1/_2$ transition. The measured splitting between these features ($\Delta\nu \approx 650$ kHz) may be used to estimate V_{zz} through the relation $\Delta\nu = 3eQV_{zz}/[I(2I-1)h]$, where e is the electron charge, Q is the quadrupole moment, and h is Planck's constant.[12] The value obtained (2.50×10^{21} V/m^2 for $Q = -1.29 \times 10^{-24}$ cm^2)[13,14] is within 10% of the theoretical prediction in Table 1, which is the accuracy that can be expected from density functional theory.

The ^{17}O spectrum is more difficult to interpret because of the overlap of resonances from the six terminal sites and the single bridge oxygen; in addition, the ^{17}O spectrum has much higher noise because of the low isotopic enrichment (see the Supporting Information) and the long ^{17}O T_1. Nevertheless, the simulated spectrum (computed with $Q = -0.02558 \times 10^{-24}$ cm^2)[14,15] is seen to reproduce the positions and general appearance of the experimental lines. The prediction of the bridge oxygen resonance at ∼240 ppm proved to be particularly helpful for assigning the weak feature below the main resonance at ∼950 ppm. As for the ^{99}Tc case, the predicted resonances appear to be broader than the observed lines, the most likely reason being that the computed chemical shift anisotropies and asymmetry parameters are again too large.

The ^{17}O line shape is further broadened by heteronuclear couplings to ^{99}Tc. The size of the dipolar interaction can be approximated from the expression $d = \gamma_{Tc}\gamma_O h/4\pi^2 R^3_{TcO}$, with bond lengths $R_{TcO} \geq 1.649$ Å. Our calculations of the ^{99}Tc−^{17}O scalar couplings give values of −248, −157, −127, and −117 Hz for the bridge and terminal oxygens 1−3, respectively, which may be compared to the measured magnitude of 132 Hz in the pertechnetate ion.[16−18] The total contribution of heteronuclear interactions to the ^{17}O line width can be estimated to be up to 10 kHz, bearing in mind that a coupling to ^{99}Tc splits the ^{17}O resonance into a dectet. On the other hand, the heteronuclear interactions are negligible in the ^{99}Tc spectrum because of the low levels of the ^{17}O isotope in unenriched samples.

This paper has presented NMR parameters obtained by solid-state experiments and relativistic density functional theory calculations for an entire bimetallic oxide containing both bridging and nonbridging oxygens. The observed discrepancies are within the accuracy of the approximation methods used. These results suggest that the theoretical analysis used here, wherein a high-level treatment is applied to the central molecule in a finite-size environment, achieves an accuracy that will be useful for elucidating other aspects of Tc(VII) oxides, including the origins of the unusual structure and magnetic behavior of Tc_2O_7 and the chemistry of the environmentally troublesome pertechnetate ion. Further work is in progress.

Acknowledgment. The Pacific Northwest National Laboratory (PNNL) is operated for the U.S. Department of Energy (DOE) by the Battelle Memorial Institute under Contract DE-AC06-76RLO-1830. Part of the research was performed at the EMSL, a national scientific user facility sponsored by the U.S. DOE's Office of Biological and Environmental Research located at PNNL. Funding for the research performed at UNLV was provided by a subcontract through the U.S. DOE Office of Science, Office of Basic Energy Sciences, under Contract DE-SC0001798 and the U.S. DOE Office of Nuclear Energy under Contract DE-FC07-06ID14781. The authors thank Mr. Tom O'Dou (UNLV) for outstanding health physics support, Mr. Joe Gregar (Argonne) for the design of a novel Pyrex reactor used in the synthesis of Tc_2O_7, and Dr. Gordon Jarvinen (Los Alamos) for a generous loan of ammonium pertechnetate.

Supporting Information Available: Description of experimental techniques and methods, atomic coordinates of the $(Tc_2O_7)_{17}$ cluster, and computed EFG and shielding tensor data for Tc and O atoms. This material is available free of charge via the Internet at http://pubs.acs.org.

References

(1) Krebs, B.; Müller, A.; Beyer, H. H. *Inorg. Chem.* **1969**, *8*, 436–443.
(2) Krebs, B. *Angew. Chem., Int. Ed.* **1969**, *8*, 381–382.
(3) Krebs, B. *Z. Anorg. Allg. Chem.* **1971**, 146–159.
(4) Nelson, C. M.; Boyd, G. E.; Smith, W. T., Jr. *J. Am. Chem. Soc.* **1954**, *76*, 348–352.
(5) Cohen, M. H.; Reif, F. *Solid State Phys.* **1957**, 321–438.
(6) Haeberlen, U. *High Resolution NMR in Solids: Selective Averaging*; Academic Press: New York, 1976.

(7) Cho, H.; de Jong, W. A.; Soderquist, C. Z. *J. Chem. Phys.* **2010**, *132*, 084501.
(8) (a) *ADF*, version 2008.01; Scientific Computing & Modelling BV: Amsterdam, 2008; http://www.scm.com. (b) te Velde, G.; Bickelhaupt, F. M.; Baerends, E. J.; Fonseca Guerra, C.; van Gisbergen, S. J. A.; Snijders, J. G.; Ziegler, T. J. *J. Comput. Chem.* **2001**, *22*, 931–967. (c) Wolff, S. K.; Ziegler, T.; van Lenthe, E.; Baerends, E. J. *J. Chem. Phys.* **1999**, *110*, 7689–7698.
(9) van Lenthe, E.; Ehlers, A. E.; Baerends, E. J. *J. Chem. Phys.* **1999**, *110*, 8943–8953.
(10) Perdew, J. P.; Burke, K.; Ernzerhof, M. *Phys. Rev. Lett.* **1996**, *77*, 3865–3868.
(11) Klamt, A.; Schüürmann, G. *J. Chem. Soc., Perkin Trans. 2* **1993**, *5*, 799–805.
(12) Taylor, P. C.; Baugher, J. F.; Kriz, H. M. *Chem. Rev.* **1975**, *75*, 203–240.
(13) Büttgenbach, S. *Hyperfine Structure in 4d- and 5d-Shell Atoms*; Springer-Verlag: Berlin, 1982.
(14) Pyykkö, P. *Mol. Phys.* **2001**, *99*, 1617–1629.
(15) Sundholm, D.; Olsen, J. *J. Phys. Chem.* **1992**, *96*, 627–630.
(16) Buckingham, M. J.; Hawkes, G. E.; Thornback, J. R. *Inorg. Chem. Acta* **1981**, *56*, L41–L42.
(17) Tarasov, V. P.; Privalov, V. I.; Kirakosyan, G. A.; Gorbik, A. A.; Buslaev, Yu. A. *Dokl. Akad. Nauk SSSR* **1982**, *263*, 1416–1418.
(18) Cho, H.; de Jong, W. A.; McNamara, B. K.; Rapko, B. M.; Burgeson, I. E. *J. Am. Chem. Soc.* **2004**, *126*, 11583–11588.

JA105687J